S. Hafner, A. Rashidi, G. Baldea, U. Riedel
A detailed chemical kinetic model of high-temperature ethylene glycol gasification
Combustion Theory and Modelling
Volume 5, Issue 4 (2011) 517-535

http://dx.doi.org/10.1080/13647830.2010.547602

Combustion Theory and Modelling
Vol. 00, No. 00, December 2009, 1–11

RESEARCH ARTICLE

A Detailed Chemical Kinetic Model of High Temperature Ethylene Glycol Gasification

S. Hafner[a*], A. Rashidi[a], G. Baldea[a], U. Riedel[ab]

[a] *University of Heidelberg, Interdisciplinary Center for Scientific Computing (IWR), D-69120 Heidelberg, Germany*; [b] *German Aerospace Center (DLR), D-70569 Stuttgart, Germany*

(*July 2010*)

In recent experimental investigations, ethylene glycol is used as model substance for biomass based pyrolysis oil in an entrained flow gasifier. In order to get deeper insight into process sequences and to conduct parametric analysis, this study describes the development and validation of a detailed chemical kinetic model for ethylene glycol gasification. A detailed reaction mechanism based on elementary reactions has been developed considering 81 species in 1247 reactions for the application in the CFD-Software ANSYS FLUENT. In addition to mechanism validation based on laminar flame speeds, ignition delay times, and concentration profiles, simulation results are compared to experimental data of ethylene glycol gasification in complex turbulent reactive flow conditions.

Keywords: biomass; gasification; CFD; detailed chemistry; ethylene glycol

1. Introduction

Biomass, as the only renewable carbon source, will most likely substitute gradually a fraction of fossil fuels for energy, fuel, and chemical supplies. On that account at the Karlsruhe Institute of Technology (KIT) the two-stage *bioliq* process is being developed, in which straw or other abundant lignocellulosic agricultural waste-products are converted to synthesis gas through fast pyrolysis and subsequent entrained flow gasification [1]. For experimental studies with a research entrained flow gasifier (REGA) at the KIT, ethylene glycol is used as model substance for the biomass based pyrolysis oil [2]. In order to attain a better understanding of the gasification process, a detailed gasifier model is being investigated including detailed oxidation chemistry. In this study, we present a detailed reaction mechanism for the model substance ethylene glycol.

Since ethylene glycol is not commonly used under high-temperature oxidizing conditions, there is a lack of available kinetic data for mechanism development, as well as literature data for mechanism validation in the temperature range of interest. In order to develop the reaction mechanism, a previously developed $C_1 - C_4$ mechanism [3] is extended with a submechanism for ethylene glycol. For reactions with no kinetic rates documented in literature, kinetic parameters were estimated using analogy methods and Evans-Polanyi equations [4]. Mechanism validation is

*Corresponding author. Email: simon.hafner@iwr.uni-heidelberg.de

ISSN: 1364-7830 print/ISSN 1741-3559 online

DOI: 10.1080/1364783YYxxxxxxxx
http://www.informaworld.com

done by the comparison of important submechanisms of the developed mechanism with literature values of corresponding experiments for laminar flame speeds, species concentrations and ignition delay times. Further on, laminar flame speeds and ignition delay times of ethylene glycol are calculated and their validities are assessed. The main validation of the complete ethylene glycol mechanism is performed by comparing experimental species concentration profiles of a pilot scale atmospheric entrained flow gasifier [Quelle KIT oder Co-autor] with calculated species concentration profiles, using a reduced version of the ethylene glycol mechanism. ANSYS FLUENT 12.0 is used for the calculation of the turbulent reacting flow in the gasifier.

The developed ethylene glycol model could be utilized for calculating species concentration profiles and product gas compositions in order to substitute cost and time consuming gasification experiments in this specific case and in general in applications of high-temperature ethylene glycol oxidation.

2. Reaction Mechanism Development

The reaction mechanism of high-temperature ethylene glycol oxidation is described as a set of elementary reactions. Modified Arrhenius equations with a temperature dependent pre-exponential factor are used to express temperature dependence of chemical reaction rates. Pressure dependence is described with the F-Center formalism of Troe [5].

An improved version of a previously validated $C_1 - C_4$ mechanism [3], consisting of 61 species in 778 elementary reactions is used as the base mechanism for the ethylene glycol reaction scheme. This mechanism is enhanced by reactions for ethanol, taken from Marinov [6]. Reaction rate constants of reactions with ethylene glycol and its products are implemented based on experiments, similar reaction schemes or estimated using analogy methods.

The thermodynamic properties for species used in the base machanism are taken from CHEMKIN thermodynamic database [7] and Marinov's ethanol reaction scheme [6]. The thermodynamic data for ethylene glycol and its products were calculated for this study by professor Burcat and included in the *Third Millennium Ideal Gas and Condensed Phase Thermochemical Database for Combustion* [8]. The developed reaction scheme for ethylene glycol consists of 81 species in 1247 elementary reactions.

2.1 Kinetic Rate Estimation

As depicted above, no kinetic rate data for ethylene glycol and some of its intermediate reaction products are available from experiments. Therefore, the submechanism for ethylene glycol was developed relying on the hierarchical order of using literature-based kinetic data whenever possible, evaluated kinetic rate constant information or rate constant estimations based on analogies to similar reactions. The estimation of pre-exponential factors is done using statistical correlations. One example is the doubling of the pre-exponential factor of analogical ethanol reactions when estimating the H-abstraction from one hydroxyl-group of ethylene glycol.

Differences in the activation energies of analogical reactions are estimated by Evans-Polanyi equations [4]:

$$Ea_1 = Ea_0 + \alpha \Delta H_{rxn} \tag{1}$$

The influences on ethylene glycol flame velocities and ignition delay times using different values of α ($0 \leq \alpha \leq 1$) are discussed in subsection 5.

2.2 Reaction Mechanism Analysis

The in-house simulation program HOMREA [9] is used for computing time-dependent homogeneous reaction systems. The governing equations are derived from the Navier-Stokes equations and are solved numerically with either a modified DASSL [10] or a modified LIMEX [11] solver, under the assumptions of ideal gas and negligible radiative heat fluxes. In this study ignition delay times, sensitivity analysis and reaction flow analysis are performed with HOMREA.

With the computational package MIXFLA [12], developed in IWR, simulation of speed and structure of stationary premixed 1-dimensional laminar flat flames can be performed. The conservation equations for the total mass, the species masses and the enthalpy are derived, using the corresponding densities, fluxes and sources in the general form of the continuity equation. To avoid complications due to stiffness or quasi-steady assumptions, the non-stationary conservation equations for the species masses and enthalpy are solved in an implicit finite difference procedure, described in [12].

For the better understanding of the reaction system and mechanism reduction, it is essential to identify the characteristic reaction paths and rate-limiting reaction steps. For the latter, sensitivity analysis can be performed with HOMREA and MIXFLA. The rate laws for the reaction mechanism can be written as a system of first order ordinary differential equations with the rate coefficients as parameters of the system. Sensitivity coefficients for individual species are computed from the partial derivative of the species concentration with respect to the rate coefficient, keeping time constant.

The characteristic reaction paths can be found by reaction flow analysis. Here the contributions of the different reactions to the formation (or consumption) of a chemical species are considered.

Using the methods of sensitivity analysis and reaction flow analysis, mechanisms can be reduced by eliminating steps, that are irrelevant for the studied problem in the actual conditions. Mechanism reduction is necessary to keep the computation time low for gasification reactor simulation and parametric studies.

3. CFD Simulation

In order to perform a computational fluid dynamics (CFD) simulation of the gasification process, the reduced version of the developed reaction mechanism was used in the commercial CFD code ANSYS FLUENT 12.0.

CFD models of gasification processes include the description of fluid flow, heat and mass transfer and chemical reactions. The fundamental governing set of equations are the mass conservation equation, the momentum conservation equation and the energy conservation equation, as well as species conservation equation [13]. Due to turbulent nature of the flow inside the reactor, a realizable k-ε model [14] was selected for turbulence modeling. This model has the advantage of more accurately predicting the spreading rate of both planar and round jets in comparison with other k-ε models [14].

Turbulence-chemistry interactions were taken into account by using the Eddy Dissipation Concept (EDC) model [15], which allows detailed chemical mechanisms to be included in CFD calculations. It assumes that chemical reactions occur within

the smallest turbulent structures, called the fine scales. For each fine scale, the volume fraction and the time scale are calculated. In ANSYS FLUENT, combustion at fine scales is assumed to occur as a constant pressure reactor, with initial conditions taken as the current species and temperature in the cell [16]. Reactions proceed over the calculated time scales, governed by Arrhenius rates and are integrated numerically using the In Situ Adaptive Tabulation (ISAT) algorithm [17]. Due to the fact that typical chemical mechanisms are invariably stiff and their numerical integration is computationally expensive, the EDC model should be used only when the assumption of fast chemistry is invalid. ISAT is employed to dynamically tabulate the chemistry mappings and reduce the time to solution. This algorithm calculates and stores the data *in situ* rather than as a preprocessing step. Thus, only areas of the thermochemical space that are accessed are included in the database. This database is built up during the reactive flow calculation. Each entry in the table corresponds to a composition that occurs in the calculation.

The Discrete Ordinate (DO) model [18] is used to simulate the heat transfer due to radiation. The model solves the radiative transfer equation for a finite number of discrete solid angels, each associated with a vector direction fixed in the global Cartesian system, and the integral over these directions are replaced by numerical quadratures.

Due to the geometrical symmetry of the simulated field, a 2D axisymmetric geometry was used. A structured quadratic element grid with Successive Ratio scheme was generated. A first-order-upwind scheme was applied for interpolation within a pressure-based implicit solver [16]. The SIMPLE numerical scheme is used to handle the pressure and velocity coupling.

4. Results of Base Mechanism Validation

Given that there are no experimental or numerical data available for the mechanism validation of high-temperature ethylene glycol oxidation, base mechanism validation played a key role in this study. Therefore, main reaction paths of ethylene glycol decomposition were calculated to define important submechanisms for base mechanism validation. Fig. 1 shows the main reaction paths of high-temperature oxidation of ethylene glycol under fuel-rich conditions in a jet stirred reactor. The main reaction path, under this condition, was the decomposition of ethylene glycol to acetaldehyde with subsequent H-abstraction to the acetaldehyde radical CH_3CO and finally the decomposition to CH_3 and CO. Another important reaction path is the decomposition over the CH_2OH-radical to formaldehyde and subsequent reactions to CO over CHO. Generally decomposition reactions played an important role in ethylene glycol oxidation under the investigated fuel-rich conditions.

For acetaldehyde, as main intermediate product, its submechanism could be validated with literature values of concentration profiles, ignition delay times and laminar flame velocities. In addition, due to same key intermediate species (marked with grey in Fig. 1), the submechanisms of ethanol and methane were validated against literature data.

4.1 Acetaldehyde Submechanism Validation

Dagaut et al. investigated acetaldehyde ignition in shock waves in a wide range of conditions ($0.5 \leq \phi \leq 2$, 1230 - 2530 K, 3.5 - 5 atm), and ignition delay times have been documented in [19]. In the same study, a comprehensive kinetic reaction mechanism for acetaldehyde oxidation is presented. In Fig. 2, results for ignition delay

times, calculated with the submechanism for acetaldehyde are compared to ignition delay measurements and modeling results at 3.5 atm under fuel-lean (ϕ=0.5) and fuel-rich (ϕ=2) conditions. Ignition delay was indicated in our simulations, like in the experiments, by the occurrence of a maximum emission of CO_2. Good agreement was achieved, but like the ignition delay times simulated by Dagaut et al., our results showed slightly lower values compared to measurements.

Gibbs and Calcote [20] investigated laminar flame speeds of acetaldehyde-air gas mixtures at 1 atm pressure and a temperature of 298 K. In Fig. 3 it can be seen that our model underpredicts flame speed in the equivalence ratio range of 0.9 - 1.1 and overpredicts flame speeds for equivalence ratios above 1.1. However, comparative calculations with mechanisms of Chevalier [21], Karbach [22] and Nehse [23] showed the same trends with same magnitudes of deviations.

Dagaut et al. [19] determined acetaldehyde oxidation experiments in a jet stirred reactor at high temperatures (900 - 1300 K) and different pressures. Amongst other species, molecular species concentration profiles were measured for CH_3CHO, O_2, CO, CO_2, H_2 and CH_2CO using probe sampling and GC analysis. Fig. 4 and Fig. 5 show concentration profiles, calculated with our ethylene glycol mechanism, compared to experimental values of Dagaut et al. at equivalence ratios of ϕ = 0.8 and ϕ = 1.6 respectively. For both cases, values of CH_2CO concentrations were underpredicted by the simulations. For ϕ = 0.8, model predictions showed slightly lower concentrations for CO_2 below the temparature of 1250 K. Very good agreement was achieved for the other species.

4.2 Ethanol Submechanism Validation

Natarajan and Bhaskaran [24] were the first researchers to conduct experiments on the ignition of ethanol-oxygen-argon gas mixtures. Experiments were performed behind reflected shock waves under different conditions ($0.5 \leq \phi \leq 2$, 1300 - 1700 K, 1 - 2 atm). For simulations, the ignition delay times were assumed to be the maximum in the product of CO and O-atom concentrations, which was taken as indicator by Marinov [6] for modeling the same experiments as well. Fig. 6 and Fig. 7 show a comparison of calculated ignition delay times with corresponding experimental values for pressures of 1 and 2 atm at stoichiometric ($\phi = 1$) and fuel-rich (ϕ = 2) conditions respectively. Calculated results showed good agreements with experiments under both conditions. A comparison of simulated results with experiments for lean conditions and experimental results of Dunphy and Simmie [25] were conducted but not presented in this work. Simulated ignition delay times for these experiments showed equal or better agreements with experiments.

Gülder [26] performed laminar flame speed measurements of ethanol-air gas mixtures in a constant volume bomb at different pressure and temperature conditions. He reported a maximum uncertainty of $\pm$2.0 cm/sec for the measured laminar flame speeds and $\pm$0.015 for the equivalence ratios. Egolfopoulos et al. [27] used the counterflow twin-flame technique to measure laminar flame speeds at 1 atm pressure and different temperatures. They reported a maximum uncertainty of $\pm$10% to their measured flame speeds. In Fig. 8 simulated flame speeds with the ethylene glycol mechanism at 1 atm pressure and a temperature of 298 K are compared to experimental values of Gülder and Egolfopoulos et al. In the 1.3 - 1.5 equivalence ratio range, the simulated flame speeds show a slight overprediction. Very good agreement with experimental data was achieved at the other equivalence ratios.

To determine species concentrations, Aboussi [28] investigated ethanol oxidation experiments in a jet-stirred reactor. The experimental conditions covered the 1000 - 1200 K temperature range, and equivalence ratios between 0.2 and 2.0 at a fixed

ethanol concentration of 0.3%. In Fig. 9 and Fig. 10 numerical results with the ethylene glycol mechanism were compared to experimental data at equivalence ratios of 1.0 and 2.0 respectively. The examined species were C_2H_5OH, CH_3CHO, C_2H_4, CH_4, CO_2 and CO. Simulated results showed good agreements with experiments as the mean residence time was varied. Merely the ethylene glycol model overpredicted concentrations of CH_3CHO and CO_2 for stoichiometric conditions while concentrations of CH_3CHO were overpredicted and concentrations of CO were underpredicted in the fuel-rich case. Good agreement was achieved for the other species.

4.3 Methane Submechanism Validation

For the validation of the methane submechanism, experiments of Cooke et al. (ϕ = 2, 1700 - 2400 K, 0.26 - 0.39 bar) [29], Suzuki et al. (ϕ = 1, 1400 - 2100 K, 1.5 - 3.5 bar) [30] and Tsuboi and Wagner (ϕ = 0.2, 1600 - 2000 K, 12.4 - 15 bar) [31] were considered. Calculated ignition delay times with the ethylene glycol mechanism, illustrated in Fig. 11 showed good agreements with experimentally determined ignition delay times.

Calculated laminar flame speeds of methane-air mixtures were validated against experimental values of van Maaren [32], Egolfopoulos [33] and Vagelopoulos [34]. As can be seen from Fig. 12, calculated laminar flame speeds showed slightly lower values for the equivalence ratio range of 1.0 - 1.15 and slightly higher values for equivalence ratios greater than 1.3.

4.4 Summary of Base Mechanism Validation

In general, regarding the validation of the acetaldehyde, ethanol and methane submechanisms, simulated results for ignition delay times, laminar flame speeds and species concentration profiles were in an acceptable deviation range with respect to experimental data. For laminar flame speeds, calculated flame speeds, by trend, seemed to be slightly overpredicted at fuel-rich conditions. In addition, no general trends for ignition delay times or concentration profiles could be deduced from submechanism validation.

5. Results of Ethylene Glycol Calculations

As discussed previously, no experimental data are available for ethylene glycol mechanism validation with laminar flame speeds and high-temperature ignition delay times. Hence, for ignition delay times and laminar flame speeds, simulated results were compared to experiments of ethanol oxidation and ethane oxidation. Concentration profiles were validated against experimental data from a research entrained flow gasifier, investigated at the Karlsruhe Institute of Technology [Quelle? oder Co-autor?].

D'Onofrio [35] investigated ignition delay times for ethylene glycol in the temperature range of 613 - 713 K. The trend of ignition delay times was extrapolated to high temperatures assuming a linear progression of the logarithmic ignition delay time versus inverted temperature. This estimation could only be used as a very rough evaluation. Additionally, experimental values of ethanol from Egolfopoulos are shown in Fig. 13 for visualizing the order of magnitude of ethylene glycol ignition delay times. From Fig. 13 it can be seen, that ignition delay times of ethylene glycol were in the same order of magnitude as ethanol ignition delay times under

same conditions. The comparison of extrapolated data from low temperature range showed quite good agreement.

The fine solid lines show error tolerances of ethylene glycol ignition delay times due to the estimation of rate parameters with Evans-Polanyi equations. Slower ignition delay times resulted from α-values greater than 0.5 and vice versa with α-values smaller than 0.5. In Fig. 13, the α-values used were 0.0, 0.5 and 1.0.

Sensitivity analysis were performed for ignition delay times of ethylene glycol at atmospheric pressure and a temperature of 1500 K. The calculations were done for fuel-lean, stoichiometric, and fuel-rich conditions using fuel-oxygen mixtures of 10 % diluted in 90 % argon. It can be seen in Fig. 14, that in addition to the $H + O_2 \rightarrow O + OH$ and $HO_2 + OH \rightarrow H_2O + O_2$ reactions, the decomposition reactions of ethylene glycol (EthGly + M) to $CH_2OH + CH_2OH + M$, $OH + CH_2CH_2OH + M$ and $H_2O + CH_3CHO + M$ played dominant roles for the values of ignition delay times. Furthermore the reactions of ethylene glycol with OH and HO_2 to $R - CH_2O + H_2O$ and $H_2O_2 + R - CHOH$ respectively, showed high sensitivities for ignition delay times.

In Fig. 15 laminar flame speeds, calculated for ethylene glycol at atmospheric pressure and a temperature of 298 K, are compared to experimental data of ethanol and ethane at same conditions. At equivalence ratios below 1.1, flame speeds of ethylene glycol showed same characteristics as flame speeds of ethane and ethanol. For equivalence ratios greater than 1.1, calculated flame speeds were higher than the experimental results for ethane and ethanol. Gibbs and Calcote [20] studied effects of molecular structure on flame speeds. For the substitution of a H-radical with an OH-group, they reported increasing flame speeds. This trend could also be confirmed by comparing more recent experimental data of flame speeds of ethane [36] and ethanol [27], which could also be seen in Fig. 15. Furthermore, the comparison of experimentally determined flame speeds of methanol [26] with data for methane [32–34] showed the same trend. Consequentially, the additional H-radical substitution by an OH-radical in ethylene glycol compared to ethanol was expected to lead to higher flame velocities. This trend was confirmed by our calculations for equivalence ratios greater than 1.1, but these higher flame speeds should be reviewed critically. Indeed, the comparison of methane and methanol flame speeds showed higher influences of the OH-group on flame speeds at fuel-rich conditions, but this trend was not observed in the comparison of ethane and ethanol flame speeds. Furthermore these trends of overpredicted flame speeds at fuel-rich conditions could also be seen from base mechanism validation, as discussed previously. This led to the assumption that laminar flame speeds, calculated with the developed ethylene glycol mechanism, are slightly overpredicted for equivalence ratios higher than 1.1.

The fine solid lines in Fig. 15 show error tolerances of ethylene glycol ignition delay times regarding the estimation of rate parameters with Evans-Polanyi equations. Slower flame speeds resulted from α-values smaller than 0.5 and vice versa with α-values greater than 0.5. In Fig. 15, the α-values used were 0.0, 0.5 and 1.0. As can be seen, the influence of different α-values on laminar flame speeds is small.

Sensitivity analysis was performed for laminar flame speeds of ethylene glycol at atmospheric pressure and a temperature of 298 K. The calculations were done for fuel-lean, stoichiometric, and fuel-rich conditions. Fig. 16 show that the $H + O_2 \rightarrow O + OH$, $HO_2 + H \rightarrow O_2 + H_2$, and $OH + CO \rightarrow H + CO_2$ reactions were the most sensitive ones to laminar flame speeds, followed by reactions with CHO and HO_2. Reactions with ethylene glycol, which were only important at fuel-rich conditions are of minor importance for laminar flame speeds compared to their influence on ignition delay times. Therefore it could be assumed that the putative

overprediction of laminar flame speeds for fuel-rich conditions is caused mainly by general trends in the base mechanism rather than errors in the estimated ethylene glycol reactions.

6. CFD Simulation Results

For the numerical simulation of the gasification process in an entrained flow gasifier using the reduced version of the developed reaction mechanism scheme, a case was considered, in which ethylene glycol was injected with a flow rate of 9.5 kg/h and gasified under fuel-rich condition ($\phi = 2.33$) and atmospheric pressure. The oxidizing agent was a mixture of air and pure oxygen (40%vol O_2). The reactor wall was kept at a constant temperature of 1373 K. The lab-scale gasifier is described in [37] in detail.

Fig. 17 shows the mole fractions of CO_2 and CO in percentage of gas volume for different distances from the burner head across the axis of symmetry of the gasifier. The experimental values are reported in [37]. As can be seen in Fig. 17, the CO_2 concentration is slightly underpredicted and the CO concentration far from the burner is overpredicted by the model. In general, the simulation results show acceptable agreement with experimental values.

7. Summary

A detailed reaction mechanism describing high temperature oxidation and decomposition of ethylene glycol has been set up. Validity of the mechanism has been tested with experimental data of laminar flame speeds, ignition delay times and concentration profiles. Due to the lack of experimental data for ethylene glycol in high temperature oxidizing conditions, key intermediate species had been determined using reaction flow analysis for the validation. For acetaldehyde, ethanol and methane its submachanisms showed good validity to experimental laminar flame speeds, ignition delay times and concentration profiles. The developed ethylene glycol mechanism was applied in simulations of an entrained flow gasification process. The comparison of experimentally determined concentration profiles with simulated results showed good agreements. Validity of the developed mechanism can be assumed until further notice since it's simulation results were tested against all relevant literature values of the currently available experimental data. But in order to further enhance reliability of simulated results with the developed mechanism, it is recommended to validate the mechanism for ethylene glycol oxidation with more experimental results conducted in ethylene glycol oxidation experiments. The presented reaction mechanism will be applied for parametric studies of entrained flow gasification, discussed in future publications.

Acknowledgments

The authors would like to thank the German Federal Ministry of Education and Research (BMBF) for the financial support of the project (Grant Nr. 03SF0320D) and also the project partners from Karlsruhe Institute of Technology for providing relevant experimental data.

References

[1] E. Henrich, N. Dahmen, K. Raffelt, R. Stahl, and F. Weirich. *The Karlsruhe "bioliq" process for biomass gasification.* In *2nd European Summer School on Renewable Motor Fuels*, 2007.

[2] U. Santo, D. Kuhn, H.J. Wiemer, E. Pantouflas, N. Zarzalis, H. Seifert, and T. Kolb. *Erzeugung von Synthesegas aus biomassestämmigen Slurries im Flugstromvergaser.* Chemie Ingenieur Technik, 79 No.5:651–656, 2007.

[3] C. Heghes. *C_1 - C_4 Hydrocarbon oxidation mechanism.* Ph.D Thesis, Heidelberg University, 2006.

[4] M.G. Evans and M. Polanyi. *Inertia and driving force of chemical reactions.* Trans. Faraday Soc., 34:11–24, 1938.

[5] R.G. Gilbert, K. Luther, and J. Troe. *Theory of unimolecular reactions in the fall-off range.* Ber. Bunsenges. Phys. Chem., 87:169, 1983.

[6] N.M. Marinov. *A detailed chemical kinetic model for high temperature ethanol oxidation.* International Journal of Chemical Kinetics, 31(3):183–220, 1999.

[7] R.J. Kee, F.M. Rupley, and J.A. Miller. *Chemkin thermodynamic data base.* Technical report, Department of Commerce, Washington DC, 1987.

[8] E. Goos, A. Burcat, B. Ruscic. *Ideal Gas Thermochemical Database with updates from Active Thermochemical Tables.* ftp://ftp.technion.ac.il/pub/supported/aetdd/thermodynamics;15-Jun-2010. mirrored at http://garfield.chem.elte.hu/Burcat/burcat.html;15-Jun-2010.

[9] U. Maas. *Mathematische Modellierung instationärer Verbrennungsprozesse unter Verwendung detaillierter Reaktionsmechanismen.* Ph.D Thesis, Heidelberg University, 1988.

[10] L.R. Petzold. *Sandia national laboratories report SAND82-8637.* Technical report, Sandia National Laboratories, 1982.

[11] P. Deuflhard, E. Hairer, and J. Zugck. Technical report 318. Sonderforschungsbereich 123, Heidelberg University, 1985.

[12] J. Warnatz. *Calculation of the structure of laminar flat flames I: Flame velocity of freely propagating ozone decomposition flames.* Ber. Bunsenges. Phys. Chem., 82:193, 1978.

[13] J. Warnatz, U. Maas, and R.W. Dibble. *Combustion.* Heidelberg: Springer Verlag, 2006.

[14] T.H. Shih, W.W. Liou, A. Shabbir, Z. Yang, and J. Zhu. *A new k-ε eddy viscosity model for high reynolds number turbulent flows.* Computers Fluids, 24(3):227–238, 1995.

[15] B.F.+Magnussen. *On the structure of turbulence and a generalized eddy dissipation concept for chemical reaction in turbulent flow.* In *19th AIAA Meeting*, 1981.

[16] ANSYS FLUENT 12.0, Theory Guide, 2009.

[17] S.B. Pope. *Computationally efficient implementation of combustion chemistry using in situ adaptive tabulation.* Combust. Theory Modelling, 1:41–63, 1997.

[18] W.A. Fiveland. *Discrete ordinate methods for radiative heat transfer in isotropically and anisotropically scattering media.* Journal of Heat Transfer, 109:807–812, 1987.

[19] P. Dagaut, M. Reuillon, D. Voisin, M. Cathonnet, M. McGuinness, J.M. Simmie. *Acetaldehyde oxidation in a JSR and ignition in shock waves: Experimental and comprehensive kinetic modeling.* Combustion Science and Technology, 107:4,301–316, 1995.

[20] G.J. Gibbs and H.F. Calcote. *Effect of molecular structure on burning velocity.* J. Chem. Eng. Data, 4 (3):226–237, 1959.

[21] C. Chevalier. *Entwicklung eines detaillierten Reaktionsmechanismus zur Modellierung der Verbrennungsprozesse von Kohlenwasserstoffen bei Hoch- und Niedertemperaturbedingungen.* Ph.D Thesis, Stuttgart University, 1993.

[22] V. Karbach. *Aktualisierung und Validierung eines detaillierten Reaktionsmechanismus zur Oxidation von Kohlenwasserstoffen bei hohen Temperaturen..* Ph.D Thesis, Heidelberg University, 1997.

[23] M. Nehse. *Automatische Erstellung von detaillierten Reaktionsmechanismen zur Modellierung der Selbstzündung und laminarer Vormischflammen von gasförmigen Kohlenwasserstoff-Mischungen..* Ph.D Thesis, Heidelberg University, 2001.

[24] K. Natarajan and K.A. Bhaskaran. *An experimental and analytical investigation of high temperature ignition of ethanol.* In *Thirteenth International Shock Tube Symposium; Niagara Falls*, 834, 1981.

[25] M.P. Dunphy, P.M. Patterson, and J.M. Simmie. *High-temperature oxidation of ethanol. part 2. kinetic modelling.* J. Chem. Soc., Faraday Trans., 87:2549–2559, 1991.

[26] Ö.L. Gülder. *Laminar burning velocities of methanol, ethanol and isooctane-air mixtures.* Proceedings of the Combustion Institute 19:275–281, 1982.

[27] F.N. Egolfopoulos, D.X. Du, and C.K. Law. *A study on ethanol oxidation kinetics in laminar premixed flames, flow reactors, and shock tubes.* Proceedings of the Combustion Institute 24:833-841, 1992.

[28] B. Aboussi. Ph.D Thesis, University of Orleans, 1991.

[29] D.F. Cooke, M.G. Dodson, and A. Williams. *A shock-tube study of the ignition of methanol and ethanol with oxygen.* Combustion and Flame 16:233-236, 1971.

[30] A. Suzuki, T. Inomata, H. Jinno, and T. Moriwaki. *Effect of Bromotrifluoromethane on the ignition in methane and ethane-oxygen-argon mixtures behind shock waves.* Bull. Chem. Soc. Jpn. 64:3345-3354, 1991.

[31] T. Tsuboi and H.G Wagner. *Homogeneous thermal oxidation of methane in reflected shock waves.* Proceedings of the Combustion Institute 15:883-890, 1975.

[32] A. van Maaren and L.P.H. de Goey. *Strech and the adiabatic burning velocity of methane- and propane-air flames.* Combustion Science and Technology 102:309-314, 1994.

[33] F.N. Egolfopoulos, D.L. Zhu, and C.K. Law. *Experimantal and numerical determination of laminar flame speeds: Mixtures of C_2-hydrocarbons with oxygen and nitrogen.* Proceedings of the Combustion Institute 23:471–478, 1990.

[34] C.M. Vagelopoulos and F.N. Egolfopoulos. *Laminar flame speeds and extinction strain rates of mixtures of carbon monoxide with hydrogen, methane and air.* Proceedings of the Combustion Institute 25:1317–1323, 1994.

[35] E.J. D'Onofrio. *Cool flame and autoignition in glycols.* Loss Prevention 13:89–97, 1979.

[36] F.N. Egolfopoulos, P. Cho, and C.K. Law. *Laminar flame speeds of methane/air mixtures under reduced and elevated pressures.* Combustion and Flame 76:375–391, 1989.

[37] A. Rashidi and U. Riedel. *CFD simulation of gasification process with ethylene glycol as model substance for biomass based pyrolysis oil.* In *10th Conference on Energy for a Clean Environment*, 2009.

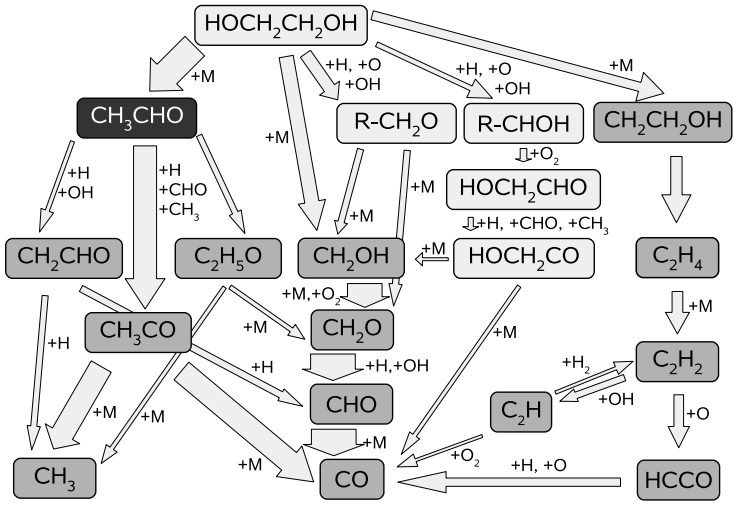

Figure 1. Reaction Flow Analysis of Ethylene Glycol Oxidation (4.45% Ethylene Glycol, 5.55% O_2, 90% Ar, p = 1 bar, T = 1700 K).

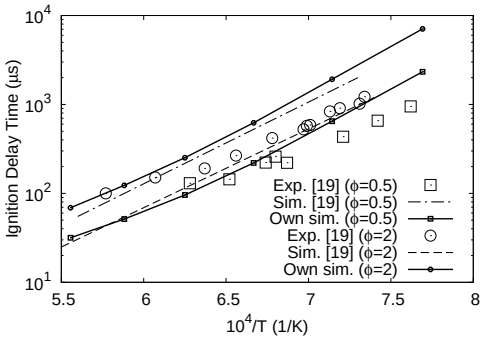

Figure 2. Experimental (exp.) and simulated (sim.) acetaldehyde ignition delay times at p = 3.5 bar.

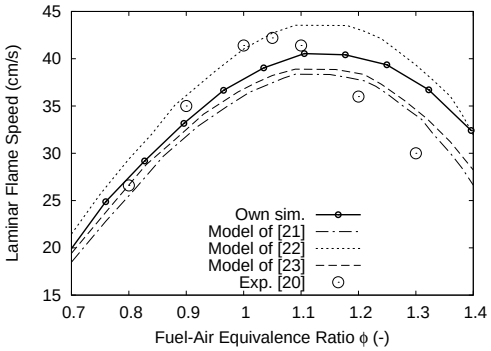

Figure 3. Experimental (exp.) and simulated (sim.) acetaldehyde laminar flame speeds at T = 298 K and p = 1 bar.

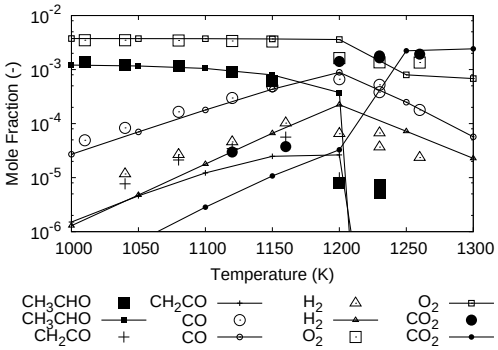

Figure 4. Experimental (points) [19] and simulated (lines) concentration profiles of acetaldehyde combustion $\phi = 0.8$, p = 1 bar.

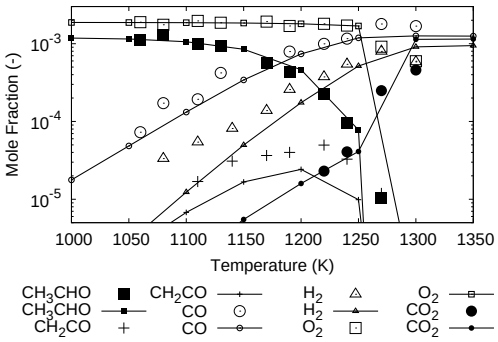

Figure 5. Experimental (points) [19] and simulated (lines) concentration profiles of acetaldehyde combustion $\phi = 1.6$, p = 1 bar.

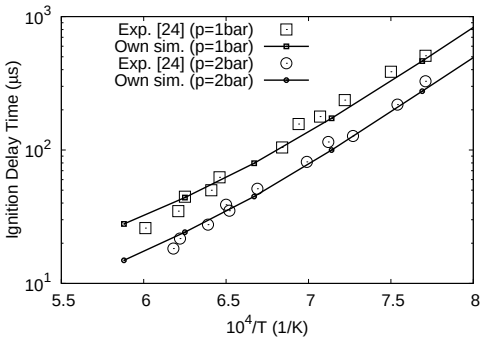

Figure 6. Experimental (exp.) and simulated (sim.) ethanol ignition delay times at $\phi = 1$.

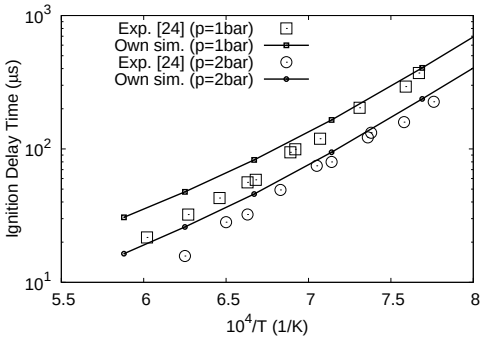

Figure 7. Experimental (exp.) and simulated (sim.) ethanol ignition delay times at $\phi = 2$.

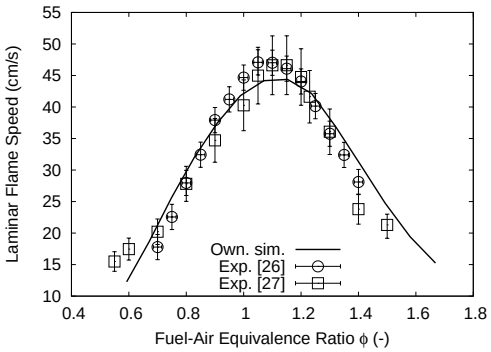

Figure 8. Experimental (exp.) and simulated (sim.) ethanol laminar flame speeds at T = 298 K and p = 1 bar.

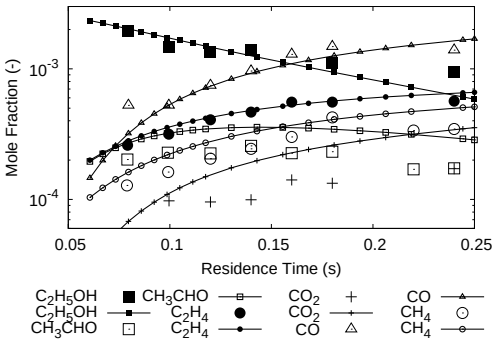

Figure 9. Experimental (points) [28] and simulated (lines) concentration profiles of ethanol combustion ϕ=0.8, p = 1 atm, T = 1056 K

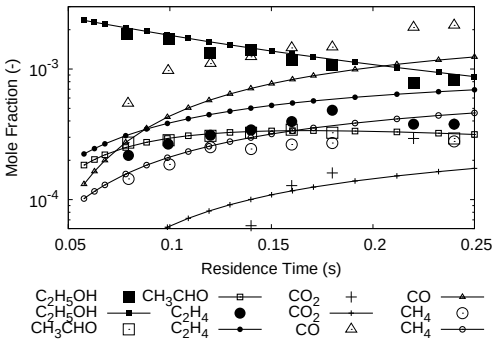

Figure 10. Experimental (points) [28] and simulated (lines) concentration profiles of acetaldehyde combustion $\phi = 1.6$, p = 1 atm, T = 1070 K

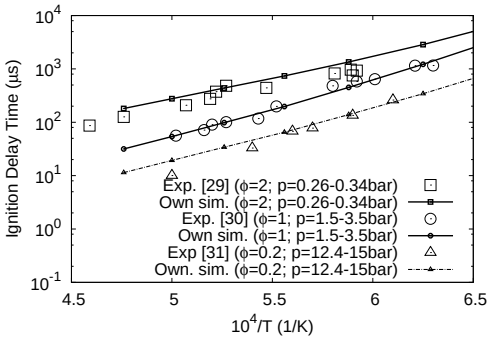

Figure 11. Experimental (exp.) and simulated (sim.) methane ignition delay times at different pressures and fuel to air ratios.

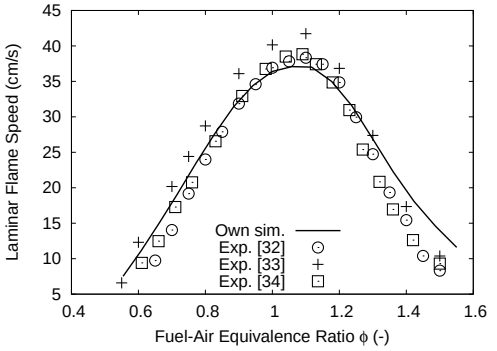

Figure 12. Experimental (exp.) and simulated (sim.) methane laminar flame speeds at T = 298 K and p = 1 bar.

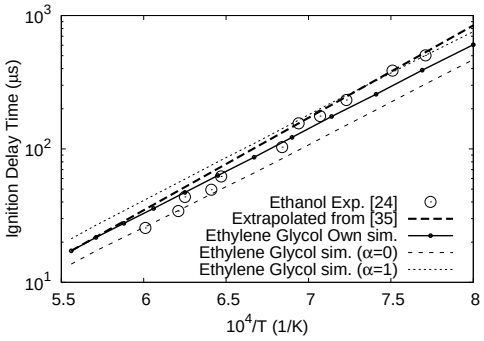

Figure 13. Simulated (sim.) ethylene glycol ignition delay times at 1bar and $\phi = 1$.

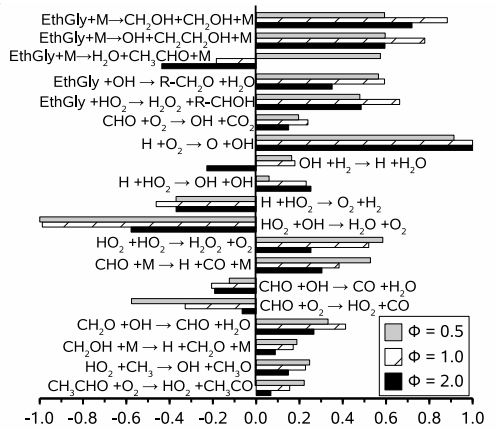

Figure 14. Normalized sensitivity coefficients of most sensitive reactions for ethylene glycol ignition delay times at p = 1 bar and $\phi = 1$.

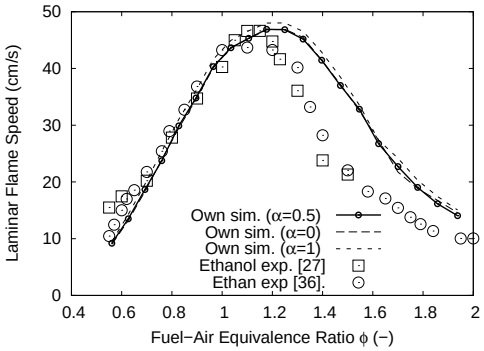

Figure 15. Experimental (exp.) and simulated (sim.) ethylene glycol laminar flame speeds at T = 298 K and p = 1 bar.

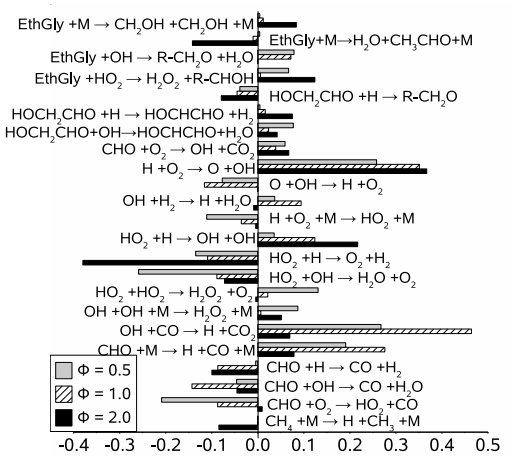

Figure 16. Normalized sensitivity coefficients of most sensitive reactions for ethylene glycol flame speeds at T = 298 K and p = 1 bar.

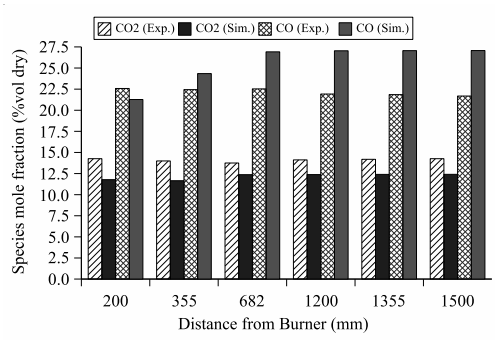

Figure 17. Experimental (exp.) and simulated (sim.) mole fractions of CO_2 and CO vs. distance from burner head.